
Calibration of Shared Equilibria in General Sum Partially Observable Markov Games

Nelson Vadori, Sumitra Ganesh, Prashant Reddy, Manuela Veloso

J.P. Morgan AI Research

{nelson.n.vadori, sumitra.ganesh, prashant.reddy, manuela.veloso}@jpmorgan.com

Abstract

Training multi-agent systems (MAS) to achieve realistic equilibria gives us a useful tool to understand and model real-world systems. We consider a general sum partially observable Markov game where agents of different types share a single policy network, conditioned on agent-specific information. This paper aims at i) formally understanding equilibria reached by such agents, and ii) matching emergent phenomena of such equilibria to real-world targets. Parameter sharing with decentralized execution has been introduced as an efficient way to train multiple agents using a single policy network. However, the nature of resulting equilibria reached by such agents has not been yet studied: we introduce the novel concept of *Shared equilibrium* as a symmetric pure Nash equilibrium of a certain Functional Form Game (FFG) and prove convergence to the latter for a certain class of games using self-play. In addition, it is important that such equilibria satisfy certain constraints so that MAS are calibrated to real world data for practical use: we solve this problem by introducing a novel dual-Reinforcement Learning based approach that fits emergent behaviors of agents in a Shared equilibrium to externally-specified targets, and apply our methods to a n -player market example. We do so by calibrating parameters governing distributions of agent types rather than individual agents, which allows both behavior differentiation among agents and coherent scaling of the shared policy network to multiple agents.

1 Introduction

Multi-agent learning in partially observable settings is a challenging task. When all agents have the same action and observation spaces, the work of Foerster *et al.* (2016); Gupta *et al.* (2017) has shown that using a single shared policy network across all agents represents an efficient training mechanism. This network takes as input the individual agent observations and outputs individual agent actions, hence the terminology *decentralized execution*. The network is trained by collecting all n agent experiences simultaneously and treating them as distinct sequences of local observations, actions and rewards experienced by the shared policy. Since agents may have different observations at a given point in time, sharing a network still allows different actions across agents. It has also been observed in these works or in Kaushik *et al.* (2018) that one can include in the agents' individual observations some agent-specific information such as the agent index to further differentiate agents when using the shared policy, thus allowing a certain form of heterogeneity among agents.

This brings the natural question: from a game theoretic standpoint, *what is the nature of potential equilibria learnt by agents using such a shared policy?* We show here that such equilibria are symmetric pure Nash equilibria of a higher level game on the set of stochastic policies, which we call *Shared equilibria*.

The second question that follows from this new concept is then *how can we constrain Shared equilibria so that they match specific externally-specified targets?* The latter is referred to as calibration, where we calibrate input parameters of the multi-agent system (MAS) so as to match externally-specified calibration targets, typically coming from real-world observations on the emergent behaviors of agents and groups of agents. For example, MAS modeling behaviors of people in a city may require that agents in equilibria take the subway no more than some number of times a day in average. Constraints such as those previously described can be achieved by having agents of different nature, or *types*, and optimally balancing those types so as to match the desired targets on the emergent behavior of agents. For example, we may want to optimally balance people living in the suburbs vs. living inside a city so as to match the constraint on taking the subway. Even then, repeating the steps (i) pick a certain set of agent types, and (ii) train agents until equilibrium is reached and record the associated calibration loss, is prohibitively expensive.

We solve this problem by introducing a reinforcement learning (RL) agent (*RL calibrator*) whose goal is to optimally balance types of agents so as to match the calibration target, and crucially who learns jointly with RL agents learning a shared equilibrium, avoiding the issue related to repeating (i)-(ii). The result is *CALSHEQ*, a new dual-RL-based algorithm for calibration of shared equilibria to external targets. *CALSHEQ* further innovates by calibrating parameters governing distributions of agent types (called *supertypes*) rather than individual agents, allowing both behavior differentiation among agents and coherent scaling of the shared policy network to multiple agents.

Our contributions are (1) we introduce the concept of Shared equilibrium that answers the question on the nature of equilibria reached by agents of possibly different types using a shared policy, and prove convergence to such equilibria using self-play, under certain conditions on the nature of the game. (2) we introduce *CALSHEQ*, a novel dual-RL-based algorithm aimed at the calibration of shared equilibria to externally specified targets, that innovates by introducing a RL-based calibrator learning jointly with learning RL agents and optimally picking parameters governing distributions of agent types, and show through experiments that *CALSHEQ* outperforms a Bayesian optimization baseline.

Related work. Parameter sharing for agents having the same action and observation spaces has been introduced concurrently in Foerster *et al.* (2016); Gupta *et al.* (2017), and then applied successfully in the subsequent works Foerster *et al.* (2017); Kaushik *et al.* (2018); Rashid *et al.* (2018); Sukhbaatar *et al.* (2016); Sunehag *et al.* (2018). Gupta *et al.* (2017) showed that out of the their three proposed approaches, (TRPO-based) parameter sharing was the best performer. Although their work considers a cooperative setting where agents maximize a joint reward, parameter sharing is actually the only method out of their proposed three that doesn't require reward sharing, and we exploit this fact in our work. Hernandez-Leal *et al.* (2019) constitutes an excellent survey of recent work in multi-agent deep RL. The recent paper Zheng *et al.* (2020) uses a shared policy for worker agents earning individual rewards and paying tax. There, the RL-based tax planner shares some similarities with our RL calibrator, although our calibrator is responsible for optimally picking agent type distribution rather than public information observable by all agents, and updates its policy on a slower timescale so as to allow equilibria to be reached by the shared policy.

The idea of using RL to calibrate parameters of a system probably goes back to Eiben *et al.* (2007), in the context of evolutionary algorithms. As mentioned in the recent work Avegliono & Sichman (2019), there is currently no consensus on how to calibrate parameters of agent-based models. Most methods studied so far build a surrogate of the MAS Avegliono & Sichman (2019); Lamperti *et al.* (2018). The term "surrogate" is very generic, and could be defined as a model that approximates the mapping between the input parameters and some output metric of the MAS. Lamperti *et al.* (2018) studies classifier surrogates, and in contrast to the latter and other work on calibration, our work is based on a dual-RL approach where our RL calibrator learns jointly with RL agents learning an equilibrium. In our experiments, we compare our approach to a Bayesian optimization baseline that builds such a surrogate. Inverse RL Finn *et al.* (2016) could be used for calibration, but it aims at recovering unknown rewards from input expert policy: in this work we don't need the latter and assume that rewards are known for each agent type, and that the goal is to find the optimal agent type distribution.

2 Shared Equilibria in General Sum Partially Observable Markov Games

Partially Observable Markov Game setting. We consider a n -player partially observable Markov game Hansen *et al.* (2004) where all agents share the same action and state spaces \mathcal{A} and \mathcal{S} . We make no specific assumption on the latter spaces unless specifically mentioned, and denote the joint action and state as $\mathbf{a}_t := (a_t^{(1)}, \dots, a_t^{(n)})$ and $\mathbf{s}_t := (s_t^{(1)}, \dots, s_t^{(n)})$. We assume that each agent i can only observe its own states $s_t^{(i)}$ and actions $a_t^{(i)}$, hence the partial observability. To ease notational burden, we use the notation $s_t^{(i)}$ for the agents' states instead of the $o_t^{(i)}$ traditionally used in this context, since in our case the full state \mathbf{s}_t is the concatenation of agents' states.

Agent types and supertypes. In order to differentiate agents, we assign to each agent i a **supertype** $\Lambda_i \in \mathcal{S}^{\Lambda_i}$, with $\Lambda := (\Lambda_i)_{i \in [1, n]}$. At the beginning of each episode, agent i is assigned a **type** $\lambda_i \in \mathcal{S}^\lambda$ sampled probabilistically as a function of its supertype, namely $\lambda_i \sim p_{\Lambda_i}$ for some probability density function p_{Λ_i} , and initial states $s_0^{(i)}$ are sampled independently according to the distribution $\mu_{\lambda_i}^0$. This is formally equivalent to extending agents' state space to $\mathcal{S} \times \mathcal{S}^\lambda$, with a transition kernel that keeps λ_i constant throughout an episode and equal to its randomly sampled value at $t = 0$. Supertypes are convenient as they allow to think of agents in terms of distributions of agents, and not at individual level, which allows to scale the simulation in a coherent way. In this sense they can be seen as behavioral templates according to which agents can be cloned. Typically, we create groups of agents who share the same supertype, so that the number of distinct supertypes is typically much less than the number of agents. Note that in Gupta *et al.* (2017), it is mentioned that the agent index can be included in its state: this is the special case where the supertype is that number, and the type can only take one value equal to the supertype.

Rewards, state transition kernel and type-symmetry assumption. Let $z_t^{(i)} := (s_t^{(i)}, a_t^{(i)}, \lambda_i)$. At each time t , agent i receives an individual reward $\mathcal{R}(z_t^{(i)}, \mathbf{z}_t^{(-i)})$, where the vector $\mathbf{z}_t^{(-i)} := (z_t^{(j)})_{j \neq i}$. The state transition kernel $\mathcal{T} : (\mathcal{S} \times \mathcal{A} \times \mathcal{S}^\lambda)^n \times \mathcal{S}^n \rightarrow [0, 1]$ is denoted $\mathcal{T}(\mathbf{z}_t, \mathbf{s}_t')$, and represents the probability to reach the joint state \mathbf{s}_t' conditionally on agents having the joint state/action/type structure \mathbf{z}_t . We now proceed to making assumptions on the rewards and state transition kernel that we call *type-symmetry*, since they are similar to the anonymity/role-symmetry assumption in Li & Wellman (2020), which only purpose is to guarantee that the expected reward of an agent in (2) only depends on its supertype Λ_i . Specifically, we assume that \mathcal{R} is invariant w.r.t. permutations of the $n - 1$ entries of its second argument $\mathbf{z}_t^{(-i)}$, and that for any permutation ρ , we have $\mathcal{T}(\mathbf{z}_t^\rho, \mathbf{s}_t'^\rho) = \mathcal{T}(\mathbf{z}_t, \mathbf{s}_t')$, where $\mathbf{z}_t^\rho, \mathbf{s}_t'^\rho$ are the permuted vectors. In plain words, the latter guaranties that from the point of view of a given agent, all other agents are interchangeable, and that two agents with equal supertypes and policies have the same expected cumulative reward. As in Gupta *et al.* (2017), our framework contains no explicit communication among agents.

Shared policy conditioned on agent type. In the parameter sharing approach with decentralized execution Gupta *et al.* (2017); Kaushik *et al.* (2018), agents use a common policy π , which is a probability over individual agent actions $a_t^{(i)}$ given a local state $s_t^{(i)}$. This policy is trained with the experiences of all agents simultaneously, and allows different actions among agents since they have different local states. We innovate by including the agent type λ_i in the local states and hence define the shared policy over the extended agent state space $\mathcal{S} \times \mathcal{S}^\lambda$. Denoting \mathcal{X} the space of functions $\mathcal{S} \times \mathcal{S}^\lambda \rightarrow \Delta(\mathcal{A})$, where $\Delta(\mathcal{A})$ is the space of probability distributions over actions, we then define:

$$\mathcal{X} := [\mathcal{S} \times \mathcal{S}^\lambda \rightarrow \Delta(\mathcal{A})], \quad \pi(a|s, \lambda) := \mathbb{P} \left[a_t^{(i)} \in da | s_t^{(i)} = s, \lambda_i = \lambda \right], \quad \pi \in \mathcal{X}. \quad (1)$$

Note that as often done so in imperfect information games, we can add a hidden variable h in $\pi(a_t|s_t, h_{t-1}, \lambda)$ to encode the agent history of observations Gupta *et al.* (2017): to ease notational burden we do not include it in the following, but this is without loss of generality since h can always be encapsulated in the state. Due to our type-symmetry assumptions above and given that agents' initial states are sampled independently according to the distributions $\mu_{\lambda_i}^0$, we see that the expected reward of each agent i only depends on its supertype Λ_i and the shared policy π (it also depends on other agents' supertypes Λ_{-i} independent of their ordering, but since we work with a fixed supertype profile Λ for now, Λ_{-i} is fixed when Λ_i is). We will actually need the following definition, which is slightly more general in that it allows agents $j \neq i$ to use a different policy $\pi_2 \in \mathcal{X}$, where $\gamma \in [0, 1]$

is the discount factor:

$$V_{\Lambda_i}(\pi_1, \pi_2) := \mathbb{E}_{\substack{\lambda_i \sim p_{\Lambda_i}, a_t^{(i)} \sim \pi_1(\cdot | \cdot, \lambda_i) \\ \lambda_j \sim p_{\Lambda_j}, a_t^{(j)} \sim \pi_2(\cdot | \cdot, \lambda_j)}} \left[\sum_{t=0}^{\infty} \gamma^t \mathcal{R}(z_t^{(i)}, \mathbf{z}_t^{(-i)}) \right], \quad i \neq j \in [1, n], \quad \pi_1, \pi_2 \in \mathcal{X}. \quad (2)$$

$V_{\Lambda_i}(\pi_1, \pi_2)$ is to be interpreted as the expected reward of an agent of supertype Λ_i using π_1 , while all other agents are using π_2 . This method of having an agent use π_1 and all others use π_2 is mentioned in Hefli (2017) under the name "symmetric opponents form approach" (SOFA) in the context of symmetric games. Our game as we formulated it so far is not symmetric since different supertypes get different rewards, however we will see below that we will introduce a symmetrization of the game via the function \hat{V} .

What are then the game theoretic implications of agents of different types using a shared policy? Intuitively, assume 2 players are asked to submit algorithms to play chess that will compete against each other. Starting with the white or dark pawns presents some similarities as it is chess in both cases, but also fundamental differences, hence the algorithms need to be good in all cases, whatever the type (white or dark) assigned by the random coin toss at the start of the game. The 2 players are playing a higher-level game on the space of algorithms that requires the submitted algorithms to be good in all situations. This also means we will consider games where there are "good" strategies, formalized by the concept of extended transitivity in assumption 1, needed in theorem 1.

Shared policy gradient and the higher-level game \hat{V} . In the parameter sharing framework, $\pi \equiv \pi_\theta$ is a neural network with weights θ , and the gradient $\nabla_{\theta, B}^{VPG}$ according to which the shared policy π_θ is updated (where B is the number of episodes sampled) is computed by collecting all agent experiences simultaneously and treating them as distinct sequences of local states, actions and rewards $s_t^{(i)}, a_t^{(i)}, \mathcal{R}(z_t^{(i)}, \mathbf{z}_t^{(-i)})$ experienced by the shared policy Gupta *et al.* (2017), yielding the following expression under vanilla policy gradient, similar to the single-agent case:

$$\nabla_{\theta, B}^{VPG} = \frac{1}{n} \sum_{i=1}^n g_i^B, \quad g_i^B := \frac{1}{B} \sum_{b=1}^B \sum_{t=0}^{\infty} \nabla_{\theta} \ln \pi_{\theta} \left(a_{t,b}^{(i)} | s_{t,b}^{(i)}, \lambda_{i,b} \right) \sum_{t'=t}^{\infty} \gamma^{(t'-t)} \mathcal{R}(z_{t,b}^{(i)}, \mathbf{z}_{t,b}^{(-i)}) \quad (3)$$

Note that by the strong law of large numbers, taking $B = +\infty$ in (3) simply amounts to replacing the sum by an expectation over trajectories of agent i as in (2). Proposition 1 is a key observation of this paper and sheds light upon the mechanism underlying parameter sharing in (3): in order to update the shared policy, we **a)** set all agents to use the same policy π_θ and **b)** pick one agent at random and take a step towards improving its individual reward while keeping other agents on π_θ : by (4), this yields an unbiased estimate of the gradient $\nabla_{\theta, \infty}^{VPG}$. Sampling many agents at random $\alpha \sim U[1, n]$ in order to compute the expectation in (4) will yield a less noisy gradient estimate but will not change its bias. In (4), \hat{V} is to be interpreted as the utility received by a randomly chosen agent behaving according to π_1 while all other agents behave according to π_2 .

Proposition 1. *For a function $f(\theta_1, \theta_2)$, let $\nabla_{\theta_1} f(\theta_1, \theta_2)$ be the gradient with respect to the first argument. We then have:*

$$\nabla_{\theta, \infty}^{VPG} = \nabla_{\theta_1} \hat{V}(\pi_\theta, \pi_\theta), \quad \hat{V}(\pi_1, \pi_2) := \mathbb{E}_{\alpha \sim U[1, n]} [V_{\Lambda_\alpha}(\pi_1, \pi_2)], \quad \pi_1, \pi_2 \in \mathcal{X} \quad (4)$$

where $\mathbb{E}_{\alpha \sim U[1, n]}$ indicates that the expectation is taken over α random integer in $[1, n]$.

Proof. It is known (although in a slightly different form in Lockhart *et al.* (2019) or Srinivasan *et al.* (2018) appendix D) that the term g_i^∞ in (3) is nothing else than $\nabla_{\theta_1} V_{\Lambda_i}(\pi_\theta, \pi_\theta)$, that is the sensitivity of the expected reward of an agent of supertype Λ_i to changing its policy while all other agents are kept on π_θ , cf. (2). The latter can be seen as an extension of the likelihood ratio method to imperfect information games, and allows us to write concisely, using (3):

$$\nabla_{\theta, \infty}^{VPG} = \frac{1}{n} \sum_{i=1}^n \nabla_{\theta_1} V_{\Lambda_i}(\pi_\theta, \pi_\theta) = \nabla_{\theta_1} \frac{1}{n} \sum_{i=1}^n V_{\Lambda_i}(\pi_\theta, \pi_\theta) = \nabla_{\theta_1} \mathbb{E}_{\alpha \sim U[1, n]} [V_{\Lambda_\alpha}(\pi_\theta, \pi_\theta)] \quad \square$$

Shared Equilibria. We remind Duersch *et al.* (2012) that a 2-player game is said to be symmetric if the utility received by a player only depends on its own strategy and on its opponent's strategy, but not on the player's identity, and that a pure strategy Nash equilibrium (π_1^*, π_2^*) is said to be symmetric if

$\pi_1^* = \pi_2^*$. For such games, due to symmetry, we call **payoff**(π_1, π_2) the utility received by a player playing π_1 while the other player plays π_2 .

Equation (4) suggests that the shared policy is a Nash equilibrium of the 2-player symmetric game with payoff \hat{V} , where by our definition of the term "payoff", the first player receives $\hat{V}(\pi_1, \pi_2)$ while the other receives $\hat{V}(\pi_2, \pi_1)$. This is because $\nabla_{\theta_1} \hat{V}(\pi_\theta, \pi_\theta)$ in (4) corresponds to trying to improve the utility of the first player while keeping the second player fixed, starting from the symmetric point (π_θ, π_θ) . If no such improvement is possible, we are facing by definition a symmetric Nash equilibrium, since due to symmetry of the game, no improvement is possible either for the second player starting from the same point (π_θ, π_θ) . The game with payoff \hat{V} can be seen as an abstract game (since the 2 players are not part of the n agents) where each element of the strategy set (that is, every pure strategy) is a policy $\pi \in \mathcal{X}$ defined in (1). This type of game has been introduced in Balduzzi *et al.* (2019) as a *Functional Form Game* (FFG), since pure strategies of these games are stochastic policies themselves (but of the lower-level game among the n agents). This motivates the following definition.

Definition 1. (Shared Equilibrium) A shared (resp. ϵ -shared) equilibrium π^* associated to the supertype profile Λ is defined as a pure strategy symmetric Nash (resp. ϵ -Nash) equilibrium (π^*, π^*) of the 2-player symmetric game with pure strategy set \mathcal{X} and payoff \hat{V} in (4).

Note that the previously described mechanism **a)-b)** occurring in parameter sharing is exactly what is defined as **self-play** in Balduzzi *et al.* (2019) (algorithm 2), but for the game of definition 1 with payoff \hat{V} . That is, we repeat the following steps for iterations n (i) set all agents on π_{θ_n} (ii) pick one agent at random and improve its reward according to the gradient update (4), thus finding a new policy $\pi_{\theta_{n+1}}$. The natural question is now *under which conditions do Shared equilibria exist, and can the self-play mechanism in (4) lead to such equilibria?* We know Balduzzi *et al.* (2019) that self-play is related to transitivity in games, so to answer this question, we introduce a new concept of transitivity that we call *extended transitivity* as it constitutes a generalization to 2-player symmetric general sum games of the concept of transitivity for the zero-sum case in Balduzzi *et al.* (2019). There, such a transitive game has payoff $u(x, y) := t(x) - t(y)$. One can observe that this game satisfies extended transitivity in assumption 1 with $\delta_\epsilon := \epsilon$ and $T(x) := t(x)$. Note also that their monotonic games for which $u(x, y) := \sigma(t(x) - t(y))$ (where σ is increasing) satisfy extended transitivity as well with $\delta_\epsilon := \sigma^{(-1)}(\epsilon + \sigma(0))$ and $T(x) := t(x)$.

Assumption 1. (extended transitivity) A 2-player symmetric game with pure strategy set S and payoff u is said to be extended transitive if there exists a bounded function T such that:

$$\forall \epsilon > 0, \exists \delta_\epsilon > 0 : \forall x, y \in S : \text{if } u(y, x) - u(x, x) > \epsilon, \text{ then } T(y) - T(x) > \delta_\epsilon.$$

The intuition behind assumption 1 is that T can be seen as the game "skill" that is being learnt whenever a player finds a profitable deviation from playing against itself. It will be required in theorem 1 to prove the existence of shared equilibria, which is the main result of this section. Actually, it will be proved that such equilibria are reached by following self-play previously discussed, thus showing that policy updates based on (4) with per-update improvements of at least ϵ achieve ϵ -shared equilibria within a finite number of steps. In order to do so, we need definition 2 of a *self-play sequence*, which is nothing else than a rigorous reformulation of the mechanism occurring in self-play Balduzzi *et al.* (2019) (algo 2). For ϵ -shared equilibria, assumption 1 is sufficient, but for shared equilibria, we need the continuity result in lemma 1.

Definition 2. A (f, ϵ) -self-play sequence $(x_n, y_n)_{0 \leq n \leq 2N}$ of size $0 \leq 2N \leq +\infty$ generated by $(z_n)_{n \geq 0}$ is a sequence such that for every n , $x_{2n} = y_{2n} = z_n$, $(x_{2n+1}, y_{2n+1}) = (z_{n+1}, z_n)$ and $f(x_{2n+1}, y_{2n+1}) > f(x_{2n}, y_{2n}) + \epsilon$.

Lemma 1. Assume that the rewards \mathcal{R} are bounded, and that S , \mathcal{A} and S^λ are finite. Then V_{Λ_i} is continuous on $\mathcal{X} \times \mathcal{X}$ for all i , where \mathcal{X} is equipped with the total variation metric.

Theorem 1. Let Λ be a supertype profile. Assume that the symmetric 2-player game with pure strategy set \mathcal{X} and payoff \hat{V} is extended transitive. Then, there exists an ϵ -shared equilibrium for every $\epsilon > 0$, which further can be reached within a finite number of steps following a (\hat{V}, ϵ) -self-play sequence. Further, if S , \mathcal{A} and S^λ are finite and the rewards \mathcal{R} are bounded, then there exists a shared equilibrium. In particular, if $(\pi_{\theta_n})_{n \geq 0}$ is a sequence of policies obtained following the gradient update (4) with $\hat{V}(\pi_{\theta_{n+1}}, \pi_{\theta_n}) > \hat{V}(\pi_{\theta_n}, \pi_{\theta_n}) + \epsilon$, then $(\pi_{\theta_n})_{n \geq 0}$ generates a finite (\hat{V}, ϵ) -self-play sequence and its endpoint $(\pi_\epsilon, \pi_\epsilon)$ is an ϵ -shared equilibrium.

We should comment on the relationship between our extended transitivity and potential games Monderer & Shapley (1996). In 2-player symmetric exact potential games, the deviation $u(y, z) - u(x, z)$ is equal to that of the so-called potential $P(y, z) - P(x, z)$ for all x, y, z . The first observation is that extended transitivity links increments of u and T only when improving from a symmetric point (x, x) , which isn't as restrictive as in the case of potential games. This motivates us to briefly introduce the (new, to the best of our knowledge) concept of piecewise potential game below. We start by observing that in the 2-player symmetric case, a potential can be defined as a symmetric function (i.e. $P(x, y) = P(y, x)$) such that $u(y, z) - u(x, z) = P(y, z) - P(x, z)$ for all x, y, z . So in some way, the potential increment plays the role of the "derivative" of u . We can generalize this observation to piecewise derivatives: define $x \leq y$ if and only if $u(x, x) \leq u(y, x)$ and $u(x, y) \leq u(y, y)$. We say that the symmetric game with payoff u is piecewise potential if there exists *symmetric* functions P_1 and P_2 such that $P_1(x, x) = P_2(x, x) =: T(x)$ for all x and:

$$\forall x \leq y: \quad u(y, x) - u(x, x) = P_1(y, x) - P_1(x, x), \quad u(y, y) - u(x, y) = P_2(y, y) - P_2(x, y).$$

Symmetric 2-player potential games satisfy the above definition with $P_1 = P_2$. If $x \leq y$, think of $P_1(y, x) - P_1(x, x) \sim \partial_+ u(x, x)$, the one-sided partial derivative from above (with respect to the first argument) and $P_2(y, y) - P_2(x, y) \sim \partial_- u(y, y)$, the one-sided partial derivative from below. For example for $x, y \in [0, 1]$, take $u(x, y) := h(x + y)g(x - y)$, with $g(z) = g_1(|z|)$ if $z \geq 0$ and $g(z) = g_2(|z|)$ otherwise, with $g_1(0) = g_2(0) = 1$. It can be shown that this game is piecewise potential with $P_j(x, y) = h(x + y)g_j(|x - y|)$ (under some conditions on g_1, g_2, h). That being said, a piecewise potential game satisfies for $x \leq y$:

$$T(y) - T(x) = \underbrace{u(y, x) - u(x, x)}_{\text{player 1 deviation}} + \underbrace{u(y, y) - u(x, y)}_{\text{player 2 deviation}} + \underbrace{P_2(x, y) - P_1(x, y)}_{\text{piecewise assumption}}$$

With the above decomposition, assumption 1 states that if y is an improvement for player 1 starting from (x, x) , then for $T(y) - T(x)$ to be large enough, we need the sum of the piecewise term and player 2's deviation to not be too negative, in which case such a game would be extended transitive.

3 Calibration of Shared Equilibria

We now turn to the question of calibration, that is of acting on the supertype profile Λ so as to match externally specified targets on the shared equilibrium. In a game that satisfies the conditions of theorem 1, agents will reach a shared equilibrium associated to Λ . For the MAS to accurately model a given real world system, we would like the emergent behavior of agents in that equilibrium to satisfy certain constraints. For example, in the n -player market setting of section 4, one may want certain market participants to average a certain share of the total market in terms of quantity of goods exchanged, or to only receive certain specific quantities of these goods.

Algorithm 1 (CALSHEQ) Calibration of Shared Equilibria

Input: learning rates $(\beta_m^{cal}), (\beta_m^{shared})$ satisfying assumption 2, initial calibrator and shared policies π_0^Λ, π_0 , initial supertype profile $\Lambda_0^b = \Lambda_0$ across episodes $b \in [1, B]$.

- 1: **while** π_m^Λ, π_m not converged **do**
 - 2: **for** each episode $b \in [1, B]$ **do**
 - 3: Sample supertype increment $\delta\Lambda^b \sim \pi_m^\Lambda(\cdot | \Lambda_{m-1}^b)$ and set $\Lambda_m^b := \Lambda_{m-1}^b + \delta\Lambda^b$
 - 4: Sample multi-agent episode with supertype profile Λ_m^b and shared policy π_m , with $\lambda_i \sim p_{\Lambda_m^b, i}, a_t^{(i)} \sim \pi_m(\cdot | \cdot, \lambda_i), i \in [1, n]$ cf. (2)
 - 5: update π_m with learning rate β_m^{shared} based on gradient (4) and episodes $b \in [1, B]$
 - 6: update π_m^Λ with learning rate β_m^{cal} based on gradient associated to (6) with episodes $b \in [1, B]$
-

The difficulty is that for every choice of Λ , one should in principle train agents until equilibrium is reached and record the associated calibration loss, and repeat this process until the loss is small enough, which is prohibitively expensive. The first observation we make is that our formulation of section 2 is general enough to accommodate the case where Λ is a distribution over supertypes: indeed, for a distribution $f(\Lambda)$, define new supertypes $\tilde{\Lambda}_i := f_i(\Lambda_i)$, where f_1 is the marginal distribution of Λ_1 (induced by f), and for $i \geq 2$, f_i is the distribution of Λ_i conditional on $(\Lambda_k)_{k \leq i-1}$

(in that case the equilibrium depends on $f(\Lambda)$). Thus, we solve this problem by introducing a RL calibrator agent with a stochastic policy, whose goal is to optimally pick Λ and who learns jointly with RL agents learning a shared equilibrium, but under a two-timescale stochastic approximation framework Konda & Tsitsiklis (2004). The latter is widely used in RL Dalal *et al.* (2018) and is well-suited to our problem as it allows the RL calibrator’s policy to be updated more slowly than the agent’s shared policy, yet simultaneously, thus giving enough time to the shared policy to approximately reach an equilibrium. In contrast, alternative methods such as the baseline we explore in our experiments - Bayesian optimization - do not offer this possibility, thus potentially leading to large moves in the supertype space which could prevent the shared policy to correctly learn an equilibrium.

The RL calibrator’s **state** is the current supertype Λ , and its **action** is a vector of increments $\delta\Lambda$ to apply to the supertypes, resulting in new supertypes $\Lambda + \delta\Lambda$, where we assume that Λ_i takes value in some subset of \mathbb{R}^d . This approach is in line with the literature on "learning to learn" Andrychowicz *et al.* (2016); Li & Malik (2016), since the goal of the RL calibrator is to learn optimal directions to take in the supertype space, given a current location. In practice, there is typically much less distinct supertypes than agents and the RL calibrator’s state and action spaces only include those distinct supertypes (agents sharing the same supertype being probabilistic clones of one another). The RL calibrator has full knowledge of the information across agents and is given K externally specified targets $f_*^{(k)} \in \mathbb{R}$ for functions of the form $f_{cal}^{(k)}((z_t)_{t \geq 0})$. Its **reward** r^{cal} will then be a weighted sum of (the inverse of) losses ℓ_k :

$$r^{cal} = \sum_{k=1}^K w_k \ell_k^{-1}(f_*^{(k)} - f_{cal}^{(k)}((z_t)_{t \geq 0})) \quad (5)$$

The result is algorithm 1, where at stage $m = 1$, the supertype profile Λ_1 is sampled across episodes b as $\Lambda_1^b \sim \Lambda_0 + \delta\Lambda^b$, with $\delta\Lambda^b \sim \pi_1^\Lambda(\cdot|\Lambda_0)$ and where we denote $\tilde{\pi}_1^\Lambda := \Lambda_0 + \pi_1^\Lambda(\cdot|\Lambda_0)$ the resulting distribution of Λ_1 . Then, we run multi-agent episodes b according to (2), each one of them with its supertype profile Λ_1^b , and record the reward r_b^{cal} , thus corresponding to the calibrator state Λ_0 , and action $\delta\Lambda^b$. The process is repeated, yielding for each episode b at stage $m \geq 2$, $\Lambda_m^b \sim \Lambda_{m-1}^b + \pi_m^\Lambda(\cdot|\Lambda_{m-1}^b)$, resulting in an distribution $\tilde{\pi}_m^\Lambda$ for Λ_m , empirically observed through the sampled $\{\Lambda_m^b\}_{b=1..B}$. As a result, the calibrator’s policy π^Λ maximizes the following objective at stage m :

$$V_{\pi_m}^{calib}(\pi_m^\Lambda) := \mathbb{E}_{\Lambda \sim \tilde{\pi}_{m-1}^\Lambda, \Lambda' \sim \pi_m^\Lambda(\cdot|\Lambda) + \Lambda, \lambda_i \sim p_{\Lambda_i'}, a_i^{(i)} \sim \pi_m(\cdot|\cdot, \lambda_i)} [r^{cal}] \quad (6)$$

If we make the approximation that the distribution $\tilde{\pi}_m^\Lambda$ is mostly driven by π_m^Λ , then updating the calibrator’s policy π_m^Λ more slowly will give enough time to the shared policy for equilibria to be approximately reached (since π_m^Λ is a distribution conditional on the previous supertype location, it is reasonable to assume that as learning progresses, it will compensate the latter and yield a distribution $\tilde{\pi}_m^\Lambda$ approximately independent from $\tilde{\pi}_{m-1}^\Lambda$, similarly to the stationary distribution of a Markov chain). This is reflected in assumption 2, standard under the two-timescale framework. The latter ensures Tamar *et al.* (2012) that π^Λ is seen as "quasi-static" with respect to π , and thus that π_m in (6) can be considered as having converged to a shared equilibrium depending on π_m^Λ . π^Λ is then updated based on (6) using a classical single-agent RL gradient update. This process ensures that π^Λ is updated smoothly during training and learns optimal directions to take in the supertype space, benefiting from the multiple locations Λ_m^b experienced across episodes.

Assumption 2. The learning rates $(\beta_m^{cal}), (\beta_m^{shared})$ satisfy $\frac{\beta_m^{cal}}{\beta_m^{shared}} \xrightarrow{m \rightarrow \frac{1}{2}\infty} 0$, as well as the Robbins-Monro conditions, that is their respective sum is infinite, and the sum of their squares is finite.

Our framework shares some similarities with the work on learning to optimize in swarms of particles Cao *et al.* (2019), since at each stage m , we have a distribution of supertypes empirically observed through the B episodes (each Λ_m^b can be seen as a particle). In the case where π^Λ is Gaussian, (6) can be seen as a Gaussian-blurred version of the pointwise objective Salimans *et al.* (2017) (i.e. the objective evaluated at a fixed Λ), which will contribute to make calibration smooth. Our setting allows us to further exploit smoothness properties of specific RL algorithms such as PPO Schulman *et al.* (2017), where a KL penalty controls the policy update.

4 Experiments in a n-player market setting

Experimental setting. We conduct experiments in a n -player market setting where merchant agents buy/sell goods from/to customers. Merchants try to attract customers and earn income by offering attractive prices to buy/sell their goods, and a merchant i cannot observe prices offered by other merchants to customers, hence the partial observability. We consider **2 distinct supertypes** for **5-10 merchant agents** (merchant 1 is assigned supertype 1 and the $n - 1$ others are assigned supertype 2), which are respectively vectors of size 12 and 11, resulting in **23 parameters** to calibrate in total. For each supertype we have i) 10 probabilities to be connected to 10 clusters of 50 customers each (500 customers in total) corresponding to transactions of various quantities, ii) the merchant’s tolerance to holding a large inventory of goods (inventory tolerance - impacting its reward function), which is 1 parameter for supertype 1, and the mean/variance of a normal random variable for supertype 2. In contrast, experimental results in Lamperti *et al.* (2018) only calibrate 8 or 12 parameters (although not in a RL context). The **calibration targets** we consider are related to i) the fraction of total customer transactions that a merchant can attract (*market share*) and ii) the distribution of individual transactions that a given merchant receives (the constraint is on 9 percentiles of the distribution, for each supertype). A detailed description of the setting/experiments is presented in the supplementary.

Baseline. There is currently no consensus on how to calibrate parameters of agent-based models Avegliano & Sichman (2019), but existing literature suggests using surrogate-based methods Lamperti *et al.* (2018). The baseline we consider here is Bayesian optimization (BO), a method that has been used for hyperparameter optimization. The latter can be considered as similar to this calibration task, and BO will allow us to periodically record the calibration loss related to a certain choice of supertype Λ , and suggest an optimal point to try next, via building a Gaussian Process-based surrogate of the MAS.

Performance metrics. We study 5 experimental settings fully described in supplementary, and evaluate our findings according to the following three criteria 1) calibrator reward in (6), quantifying the accuracy of the equilibrium fit to the target(s), 2) convergence of merchant agents’ rewards to an equilibrium and 3) smoothness of the supertype profile Λ as a function of training iterations, ensuring that equilibria is given sufficient time to be reached, cf. discussion on assumption 2 in section 3.

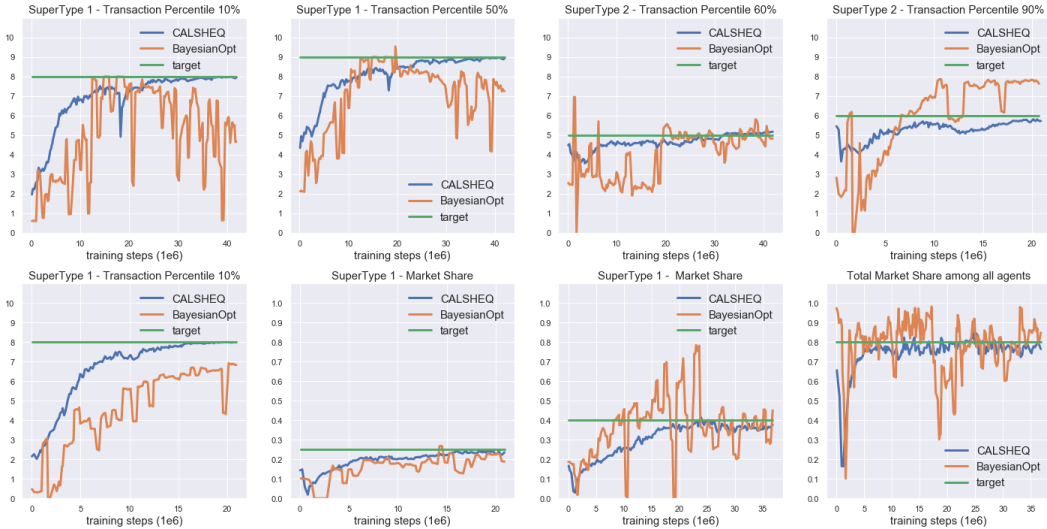


Figure 1: Calibration target fits for transaction quantity distribution percentile and Market Share during training, averaged over episodes B - Experiments 2-2-2-3 (**Top**) and 3-4-5-5 (**Bottom**) - *CALSHEQ* (ours) and baseline (Bayesian optimization).

Results. In figure 2 we display calibrator and agents’ reward evolution during training. It is seen that *CALSHEQ* outperforms BO in that i) the RL calibrator’s rewards converge more smoothly and achieve in average better results in less time, ii) in experiment 4, supertype 1’s reward in the BO case converges to a negative value, which should not happen as merchants always have the possibility to earn zero income by doing nothing. The reason for it is that as mentioned in section

3, BO can potentially perform larger moves in the supertype space when searching for a solution, whereas *CALSHEQ* uses a two-timescale framework that prevents this fact, at least in theory, and consequently merchants may not be given sufficient time to adapt to new supertype profiles Λ . This fact is further seen in figure 3 where we show supertype parameters during training (connectivity and inventory tolerance). It is seen that *CALSHEQ* smoothly varies these parameters, giving enough time for merchant agents on the shared policy to adapt, and preventing rewards to diverge as previously discussed.

The RL calibrator’s total reward in (6) is computed as weighted sum of various sub-objectives. In figure 1, we zoom on some of these individual components that constitute the overall reward, together with the associated externally specified target values (figures related to all sub-objectives of all experiments are in the supplementary). It is seen that *CALSHEQ* converges more smoothly and more accurately than BO to the target values. The considered targets are on the percentiles of the distribution of the transaction quantities received by merchants, as well as on the market share. For example, the first case considers a target of 8 for the 10% percentile of the distribution of transactions received by a merchant of supertype 1.

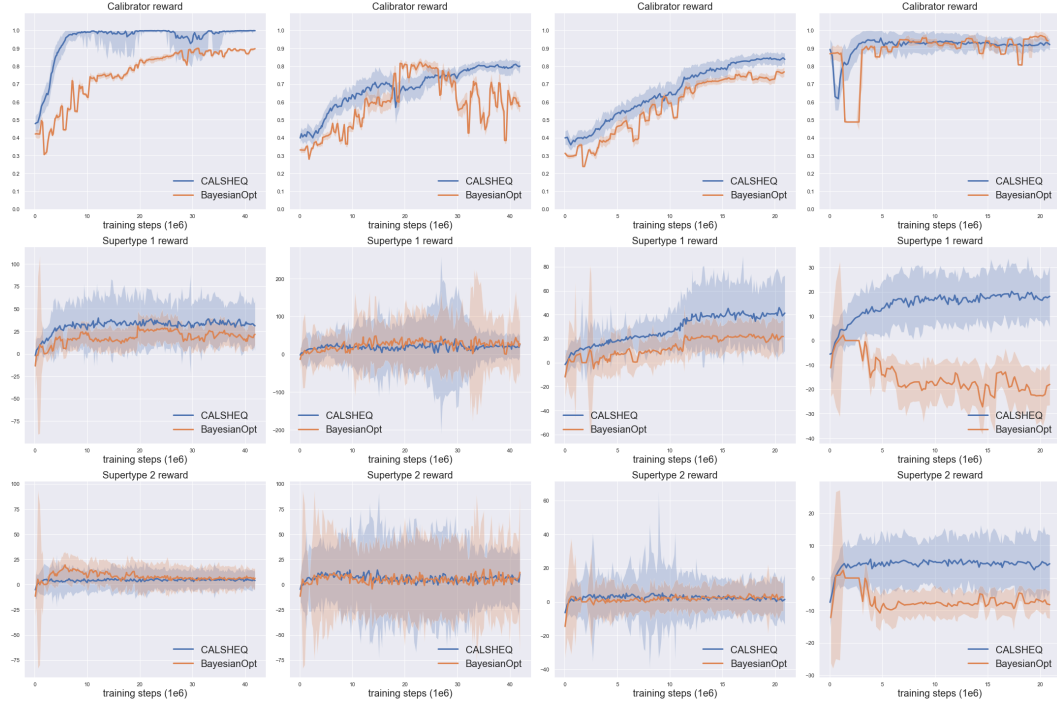


Figure 2: Rewards during training, averaged over episodes B - Calibrator (**Top**), Supertypes 1/2 (**Mid/Bottom**) - experiments 1-2-3-4. *CALSHEQ* (ours) and baseline (Bayesian optimization). Shaded area represents ± 1 stDev.

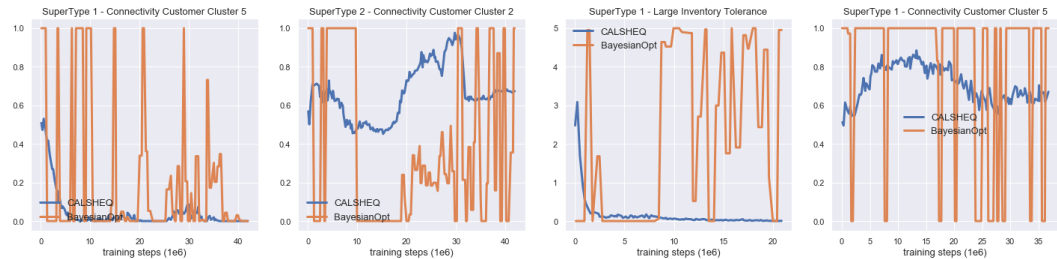


Figure 3: Smoothness of supertype parameters being calibrated during training, averaged over episodes B - Experiments 1-2-4-5 - *CALSHEQ* (ours) and baseline (Bayesian optimization).

5 Conclusion

This work was first motivated by the authors wondering what were the game theoretical implications of agents of possibly different types using a shared policy. This led to the concept of Shared equilibrium presented in this paper, which provides insight into the mechanisms underlying policy sharing. From the latter followed the natural question of how to constrain such equilibria by optimally balancing types of agents. The result is a novel dual-RL based algorithm that operates under a two-timescale stochastic approximation framework, *CALSHEQ*, for which we show through experiments that it allows to smoothly bring learning agents to equilibria satisfying certain externally specified constraints. We hope that the present work on calibration will constitute a new baseline and give further ideas to researchers attempting to constrain/calibrate equilibria learnt by learning agents.

Disclaimer

This paper was prepared for information purposes by the Artificial Intelligence Research group of JPMorgan Chase & Co and its affiliates (“JP Morgan”), and is not a product of the Research Department of JP Morgan. JP Morgan makes no representation and warranty whatsoever and disclaims all liability, for the completeness, accuracy or reliability of the information contained herein. This document is not intended as investment research or investment advice, or a recommendation, offer or solicitation for the purchase or sale of any security, financial instrument, financial product or service, or to be used in any way for evaluating the merits of participating in any transaction, and shall not constitute a solicitation under any jurisdiction or to any person, if such solicitation under such jurisdiction or to such person would be unlawful. © 2020 JPMorgan Chase & Co. All rights reserved.

References

- Andrychowicz, Marcin, Denil, Misha, Gomez, Sergio, Hoffman, Matthew W, Pfau, David, TomSchaul, Shillingford, Brendan, & Freitas, Nando De. 2016. Learning to learn by gradient descent by gradient descent. *In: Advances in Neural Information Processing Systems*.
- Avegliano, Priscilla, & Sichman, Jaime Simão. 2019. Using Surrogate Models to Calibrate Agent-based Model Parameters Under Data Scarcity. *In: AAMAS*.
- Balduzzi, David, Garnelo, Marta, Bachrach, Yoram, Czarnecki, Wojciech, Perolat, Julien, Jaderberg, Max, & Graepel, Thore. 2019. Open-ended learning in symmetric zero-sum games. *Pages 434–443 of: Chaudhuri, Kamalika, & Salakhutdinov, Ruslan (eds), Proceedings of the 36th International Conference on Machine Learning*. Proceedings of Machine Learning Research, vol. 97. Long Beach, California, USA: PMLR.
- Cao, Yue, Chen, Tianlong, Wang, Zhangyang, & Shen, Yang. 2019. Learning to Optimize in Swarms. *In: Advances in Neural Information Processing Systems*.
- Dalal, G., Szörényi, B., Thoppe, G., & Mannor, S. 2018. Finite sample analysis of two-timescale stochastic approximation with applications to reinforcement learning. *In: Proc. Conference on Learning Theory (COLT)*.
- Duersch, P., Oechssler, J., & Schipper, B.C. 2012. Pure strategy equilibria in symmetric two-player zero-sum games. *Pages 553–564 of: Int J Game Theory*, vol. 41.
- Eiben, A.E., Horvath, M., Kowalczyk, W., & Schut, M.C. 2007. Reinforcement Learning for Online Control of Evolutionary Algorithms. *Engineering Self-Organising Systems*, 151–160.
- Finn, Chelsea, Levine, Sergey, & Abbeel, Pieter. 2016. Guided Cost Learning: Deep Inverse Optimal Control via Policy Optimization. *Page 49–58 of: Proceedings of the 33rd International Conference on International Conference on Machine Learning - Volume 48. ICML’16. JMLR.org*.
- Foerster, J. N., Nardelli, N., Farquhar, G., Afouras, T., Torr, P. H. S., Kohli, P., & Whiteson, S. 2017. Stabilising Experience Replay for Deep Multi-Agent Reinforcement Learning. *In: International Conference on Machine Learning*.
- Foerster, Jakob N., Assael, Yannis M., de Freitas, Nando, & Whiteson, Shimon. 2016. Learning to Communicate with Deep Multi-Agent Reinforcement Learning. *Proceedings of the 30th International Conference on Neural Information Processing Systems*, 2145–2153.

- Gupta, Jayesh K, Egorov, Maxim, & Kochenderfer, Mykel. 2017. Cooperative Multi-agent Control Using Deep Reinforcement Learning. *Pages 66–83 of: Autonomous Agents and Multiagent Systems*. Springer International Publishing.
- Hansen, E A, Bernstein, D S, & Zilberstein, S. 2004. Dynamic programming for partially observable stochastic games. *AAAI*.
- Hefti, Andreas. 2017. Equilibria in symmetric games: theory and applications. *Theoretical Economics*, **12**, 979–1002.
- Hernandez-Leal, P., Kartal, B., & Taylor, M.E. 2019. A survey and critique of multiagent deep reinforcement learning. *Pages 750–797 of: Autonomous Agents and Multiagent Systems*. Springer International Publishing.
- Kaushik, Meha, Phaniteja, S., & Krishna, K. Madhava. 2018. Parameter Sharing Reinforcement Learning Architecture for Multi Agent Driving. *ArXiv*, **abs/1811.07214**.
- Konda, Vijay R., & Tsitsiklis, John. 2004. Convergence rate of linear two-timescale stochastic approximation. *The Annals of Applied Probability*, **14**(2), 796–819.
- Lamperti, Francesco, Roventini, Andrea, & Sani, Amir. 2018. Agent-based model calibration using machine learning surrogates. *Journal of Economic Dynamics and Control*, **90**, 366–389.
- Li, Ke, & Malik, Jitendra. 2016. Learning to Optimize. <https://arxiv.org/abs/1606.01885>.
- Li, Zun, & Wellman, Michael P. 2020. Structure Learning for Approximate Solution of Many-Player Games. *Pages 2119–2127 of: AAAI*.
- Liang, Eric, Liaw, Richard, Nishihara, Robert, Moritz, Philipp, Fox, Roy, Goldberg, Ken, Gonzalez, Joseph, Jordan, Michael, & Stoica, Ion. 2018. RLlib: Abstractions for Distributed Reinforcement Learning. *Pages 3053–3062 of: Proceedings of the 35th International Conference on Machine Learning*. Proceedings of Machine Learning Research, vol. 80.
- Lockhart, Edward, Lanctot, Marc, Pérolat, Julien, Lespiau, Jean-Baptiste, Morrill, Dustin, Timbers, Finbarr, & Tuyls, Karl. 2019. Computing Approximate Equilibria in Sequential Adversarial Games by Exploitability Descent. *In: Proceedings of the 28th International Joint Conference on Artificial Intelligence (IJCAI)*.
- Monderer, Dov, & Shapley, Lloyd S. 1996. Potential Games. *Games and Economic Behavior*, **14**, 124–143.
- Rashid, T., Samvelyan, M., de Witt, C. S., Farquhar, G., Foerster, J. N., & Whiteson, S. 2018. QMIX - Monotonic Value Function Factorisation for Deep Multi-Agent Reinforcement Learning. *In: International Conference on Machine Learning*.
- Salimans, Tim, Ho, Jonathan, Chen, Xi, & Sutskever, Ilya. 2017. Evolution Strategies as a Scalable Alternative to Reinforcement Learning. <https://arxiv.org/abs/1703.03864>.
- Schulman, John, Levine, Sergey, Abbeel, Pieter, Jordan, Michael, & Moritz, Philipp. 2015. Trust Region Policy Optimization. *Pages 1889–1897 of: Bach, Francis, & Blei, David (eds), Proceedings of the 32nd International Conference on Machine Learning*. Proceedings of Machine Learning Research, vol. 37.
- Schulman, John, Wolski, Filip, Dhariwal, Prafulla, Radford, Alec, & Klimov, Oleg. 2017. Proximal Policy Optimization Algorithms. <https://arxiv.org/abs/1707.06347>.
- Srinivas, Niranjan, Krause, Andreas, Kakade, Sham, & Seeger, Matthias. 2016. Gaussian process optimization in the bandit setting: No regret and experimental design. *ICML*.
- Srinivasan, Sriram, Lanctot, Marc, Zambaldi, Vinicius, Pérolat, Julien, Tuyls, Karl, Munos, Rémi, & Bowling, Michael. 2018. Actor-Critic Policy Optimization in Partially Observable Multiagent Environments. *In: Advances in Neural Information Processing Systems (NeurIPS)*.
- Sukhbaatar, S., Szlam, A., & Fergus, R. 2016. Learning Multiagent Communication with Backpropagation. *In: Advances in Neural Information Processing Systems*.
- Sunehag, P., Lever, G., Gruslys, A., Czarnecki, W. M., Zambaldi, V. F., Jaderberg, M., Lanctot, M., Sonnerat, N., Leibo, J. Z., Tuyls, K., & Graepel, T. 2018. Value-Decomposition Networks For Cooperative Multi-Agent Learning Based On Team Reward. *In: International Conference on Autonomous Agents and Multiagent Systems*.
- Tamar, Aviv, Di Castro, Dotan, & Mannor, Shie. 2012. Policy Gradients with Variance Related Risk Criteria. *In: ICML*.
- Zheng, Stephan, Trott, Alexander, Srinivasa, Sunil, Naik, Nikhil, Gruesbeck, Melvin, Parkes, David C., & Socher, Richard. 2020. The AI Economist: Improving Equality and Productivity with AI-Driven Tax Policies. <https://arxiv.org/abs/2004.13332>, Apr.

A Proofs

Lemma 2. *Every extended transitive game with payoff f has at least one (f, ϵ) -self-play sequence for every $\epsilon > 0$, and every such sequence is finite.*

Proof. First note that such a game has at least one (f, ϵ) -self-play sequence for every $\epsilon > 0$ since every (x, x) is a (f, ϵ) -self-play sequence of size 0 (cf. definition 2). Then, let (x_n, y_n) be a (f, ϵ) -self-play sequence. By definition of the self-play sequence we have $f(x_{2n+1}, x_{2n}) > f(x_{2n}, x_{2n}) + \epsilon$. By extended transitivity (cf. assumption 1) this implies $T(x_{2n+1}) > T(x_{2n}) + \delta_\epsilon$. But $x_{2n+1} = x_{2n+2}$ by definition of the self-play sequence, hence $T(x_{2n+2}) > T(x_{2n}) + \delta_\epsilon$. By induction $T(x_{2n}) > T(x_0) + n\delta_\epsilon$ for $n \geq 1$. If the sequence is not finite and since $\delta_\epsilon > 0$, one can take the limit as $n \rightarrow \infty$ and get a contradiction, since T is bounded by extended transitivity assumption. \square

Theorem 2. *An extended transitive game with payoff f has a symmetric pure strategy ϵ -Nash equilibrium for every $\epsilon > 0$, which further can be reached within a finite number of steps following a (f, ϵ) -self-play sequence.*

Proof. Let $\epsilon > 0$. Take a (f, ϵ) -self-play sequence. By lemma 2, such a sequence exists and is finite, hence one may take a (f, ϵ) -self-play sequence of maximal size, say $2N_\epsilon$. Assume that its end point (x, x) is not an ϵ -Nash equilibrium. Then $\exists y: f(y, x) > f(x, x) + \epsilon$, which means that one can extend the (f, ϵ) -self-play sequence to size $2N_\epsilon + 2$ with entries (y, x) and (y, y) , which violates the fact that such a sequence was taken of maximal size. \square

Theorem 3. *An extended transitive game with continuous payoff f and compact strategy set has a symmetric pure strategy Nash equilibrium.*

Proof. By theorem 2, take a sequence of ϵ_n -Nash equilibria with $\epsilon_n \rightarrow 0$ and corresponding (f, ϵ_n) -self-play sequence endpoints (x_n, x_n) . By compactness assumption, this sequence has a converging subsequence (x_{m_n}, x_{m_n}) , whose limit point (x_*, x_*) belongs to the strategy set. We have by definition of ϵ_{m_n} -Nash equilibrium that $f(x_{m_n}, x_{m_n}) \geq \sup_y f(y, x_{m_n}) - \epsilon_{m_n}$. Taking the limit as $n \rightarrow \infty$ and using continuity of f , we get $f(x_*, x_*) \geq \sup_y f(y, x_*)$, which shows that (x_*, x_*) is a symmetric pure strategy Nash equilibrium. \square

Theorem 1. Let Λ be a supertype profile. Assume that the symmetric 2-player game with pure strategy set \mathcal{X} and payoff \hat{V} is extended transitive. Then, there exists an ϵ -shared equilibrium for every $\epsilon > 0$, which further can be reached within a finite number of steps following a (\hat{V}, ϵ) -self-play sequence. Further, if \mathcal{S} , \mathcal{A} and \mathcal{S}^λ are finite and the rewards \mathcal{R} are bounded, then there exists a shared equilibrium. In particular, if $(\pi_{\theta_n})_{n \geq 0}$ is a sequence of policies obtained following the gradient update (4) with $\hat{V}(\pi_{\theta_{n+1}}, \pi_{\theta_n}) > \hat{V}(\pi_{\theta_n}, \pi_{\theta_n}) + \epsilon$, then $(\pi_{\theta_n})_{n \geq 0}$ generates a finite (\hat{V}, ϵ) -self-play sequence and its endpoint $(\pi_\epsilon, \pi_\epsilon)$ is an ϵ -shared equilibrium.

Proof. The first part of the theorem follows from theorem 2. Then, we have by assumption that \mathcal{S} , \mathcal{A} , \mathcal{S}^λ are finite. Denote $m := |\mathcal{S}| \cdot |\mathcal{A}| \cdot |\mathcal{S}^\lambda|$. In that case \mathcal{X} is given by:

$$\mathcal{X} = \{(x_a^{s,\lambda}) \in [0, 1]^m : \forall s \in [1, |\mathcal{S}|], \lambda \in [1, |\mathcal{S}^\lambda|], \sum_{a=1}^{|\mathcal{A}|} x_a^{s,\lambda} = 1\}$$

\mathcal{X} is a closed and bounded subset of $[0, 1]^m$, hence by Heine–Borel theorem it is compact. Note that closedness comes from the fact that summation to 1 is preserved by passing to the limit. By assumption, the rewards are bounded, so by lemma 1, V_{Λ_i} is continuous for all i , which yields continuity of \hat{V} , hence we can apply theorem 3 to conclude.

Finally, if $(\pi_{\theta_n})_{n \geq 0}$ is a sequence of policies obtained following the gradient update (4) with $\hat{V}(\pi_{\theta_{n+1}}, \pi_{\theta_n}) > \hat{V}(\pi_{\theta_n}, \pi_{\theta_n}) + \epsilon$, then the self-play sequence generated by $(\pi_{\theta_n})_{n \geq 0}$ is finite by lemma 2, and its endpoint is necessarily a symmetric pure strategy ϵ -Nash equilibrium according to the proof of theorem 2, hence an ϵ -shared equilibrium. \square

Lemma 1. Assume that the rewards \mathcal{R} are bounded, and that \mathcal{S} , \mathcal{A} and \mathcal{S}^λ are finite. Then V_{Λ_i} is continuous on $\mathcal{X} \times \mathcal{X}$ for all i , where \mathcal{X} is equipped with the total variation metric.

Proof. Since by assumption \mathcal{S} , \mathcal{A} and \mathcal{S}^λ are finite, we will use interchangeably sum and integral over these spaces. Let us denote the total variation metric for probability measures π_1, π_2 on \mathcal{X} :

$$\rho_{TV}(\pi_1, \pi_2) := \frac{1}{2} \max_{s, \lambda} \sum_{a \in \mathcal{A}} |\pi_1(a|s, \lambda) - \pi_2(a|s, \lambda)|$$

and let us equip the product space $\mathcal{X} \times \mathcal{X}$ with the metric:

$$\rho_{TV}((\pi_1, \pi_2), (\pi_3, \pi_4)) := \rho_{TV}(\pi_1, \pi_3) + \rho_{TV}(\pi_2, \pi_4).$$

Remember that $z_t^{(i)} := (s_t^{(i)}, a_t^{(i)}, \lambda_i)$. Let:

$$V_{\Lambda_i}(\pi_1, \pi_2, \mathbf{s}, \boldsymbol{\lambda}) := \mathbb{E}_{a_t^{(i)} \sim \pi_1(\cdot|\cdot, \lambda_i), a_t^{(j)} \sim \pi_2(\cdot|\cdot, \lambda_j)} \left[\sum_{t=0}^{\infty} \gamma^t \mathcal{R}(z_t^{(i)}, \mathbf{z}_t^{(-i)}) | \mathbf{s}_0 = \mathbf{s} \right], \quad j \neq i,$$

so that:

$$V_{\Lambda_i}(\pi_1, \pi_2) = \int_{\mathbf{s}} \int_{\boldsymbol{\lambda}} V_{\Lambda_i}(\pi_1, \pi_2, \mathbf{s}, \boldsymbol{\lambda}) \cdot \prod_{j=1}^n [\mu_{\lambda_j}^0(ds_j) p_{\Lambda_j}(d\lambda_j)]$$

Then we have:

$$\begin{aligned} V_{\Lambda_i}(\pi_1, \pi_2, \mathbf{s}, \boldsymbol{\lambda}) &= \int_{\mathbf{a}} \mathcal{R}(z^{(i)}, \mathbf{z}^{(-i)}) \pi_1(da_i|s_i, \lambda_i) \prod_{j \neq i} \pi_2(da_j|s_j, \lambda_j) \\ &+ \gamma \int_{\mathbf{a}} \int_{\mathbf{s}'} \mathcal{T}(\mathbf{z}, d\mathbf{s}') V_{\Lambda_i}(\pi_1, \pi_2)(\mathbf{s}', \boldsymbol{\lambda}) \pi_1(da_i|s_i, \lambda_i) \prod_{j \neq i} \pi_2(da_j|s_j, \lambda_j) \end{aligned}$$

The goal is to compute $|V_{\Lambda_i}(\pi_1, \pi_2, \mathbf{s}, \boldsymbol{\lambda}) - V_{\Lambda_i}(\pi_3, \pi_4, \mathbf{s}, \boldsymbol{\lambda})|$ and show that the latter is small provided that $\rho_{TV}((\pi_1, \pi_2), (\pi_3, \pi_4))$ is small. Let us use the notation:

$$c_1(\pi_1, \pi_2) := \int_{\mathbf{a}} \mathcal{R}(z^{(i)}, \mathbf{z}^{(-i)}) \pi_1(da_i|s_i, \lambda_i) \prod_{j \neq i} \pi_2(da_j|s_j, \lambda_j)$$

Since by assumption $|\mathcal{R}|$ is bounded, say by \mathcal{R}_{max} we have:

$$\begin{aligned} &|c_1(\pi_1, \pi_2) - c_1(\pi_3, \pi_4)| \\ &\leq \mathcal{R}_{max} \int_{\mathbf{a}} |\pi_1(da_i|s_i, \lambda_i) \prod_{j \neq i} \pi_2(da_j|s_j, \lambda_j) - \pi_3(da_i|s_i, \lambda_i) \prod_{j \neq i} \pi_4(da_j|s_j, \lambda_j)| \\ &\leq \mathcal{R}_{max} \int_{a_i} |\pi_1(da_i|s_i, \lambda_i) - \pi_3(da_i|s_i, \lambda_i)| \\ &+ \mathcal{R}_{max} \int_{\mathbf{a}_{-i}} |\prod_{j \neq i} \pi_2(da_j|s_j, \lambda_j) - \prod_{j \neq i} \pi_4(da_j|s_j, \lambda_j)| \\ &\leq 2\mathcal{R}_{max} \rho_{TV}(\pi_1, \pi_3) + 2\mathcal{R}_{max}(n-1) \rho_{TV}(\pi_2, \pi_4) \leq 2n\mathcal{R}_{max} \rho_{TV}((\pi_1, \pi_2), (\pi_3, \pi_4)) \end{aligned}$$

Now, let us use the notation:

$$c_2(\pi_1, \pi_2) := \int_{\mathbf{a}} \int_{\mathbf{s}'} \mathcal{T}(\mathbf{z}, d\mathbf{s}') V_{\Lambda_i}(\pi_1, \pi_2)(\mathbf{s}', \boldsymbol{\lambda}) \pi_1(da_i|s_i, \lambda_i) \prod_{j \neq i} \pi_2(da_j|s_j, \lambda_j)$$

For the term $|c_2(\pi_1, \pi_2) - c_2(\pi_3, \pi_4)|$, we can split:

$$\begin{aligned} &V_{\Lambda_i}(\pi_1, \pi_2)(\mathbf{s}', \boldsymbol{\lambda}) \pi_1(da_i|s_i, \lambda_i) \prod_{j \neq i} \pi_2(da_j|s_j, \lambda_j) \\ &\quad - V_{\Lambda_i}(\pi_3, \pi_4)(\mathbf{s}', \boldsymbol{\lambda}) \pi_3(da_i|s_i, \lambda_i) \prod_{j \neq i} \pi_4(da_j|s_j, \lambda_j) \\ &= V_{\Lambda_i}(\pi_1, \pi_2)(\mathbf{s}', \boldsymbol{\lambda}) [\pi_1(da_i|s_i, \lambda_i) \prod_{j \neq i} \pi_2(da_j|s_j, \lambda_j) - \pi_3(da_i|s_i, \lambda_i) \prod_{j \neq i} \pi_4(da_j|s_j, \lambda_j)] \\ &+ \pi_3(da_i|s_i, \lambda_i) \prod_{j \neq i} \pi_4(da_j|s_j, \lambda_j) [V_{\Lambda_i}(\pi_1, \pi_2)(\mathbf{s}', \boldsymbol{\lambda}) - V_{\Lambda_i}(\pi_3, \pi_4)(\mathbf{s}', \boldsymbol{\lambda})] \end{aligned}$$

Since V_{Λ_i} is bounded by $\mathcal{R}_{max}(1 - \gamma)^{-1}$, and noting that we have, as for c_1 , that:

$$\begin{aligned} & \int_{\mathbf{a}} |\pi_1(da_i|s_i, \lambda_i) \Pi_{j \neq i} \pi_2(da_j|s_j, \lambda_j) - \pi_3(da_i|s_i, \lambda_i) \Pi_{j \neq i} \pi_4(da_j|s_j, \lambda_j)| \\ & \leq 2n\rho_{TV}((\pi_1, \pi_2), (\pi_3, \pi_4)) \end{aligned}$$

we then have:

$$\begin{aligned} |c_2(\pi_1, \pi_2) - c_2(\pi_3, \pi_4)| & \leq 2n\mathcal{R}_{max}(1 - \gamma)^{-1}\rho_{TV}((\pi_1, \pi_2), (\pi_3, \pi_4)) \\ & \quad + \max_{\mathbf{s}, \boldsymbol{\lambda}} |V_{\Lambda_i}(\pi_1, \pi_2, \mathbf{s}, \boldsymbol{\lambda}) - V_{\Lambda_i}(\pi_3, \pi_4, \mathbf{s}, \boldsymbol{\lambda})| \end{aligned}$$

We then have, collecting all terms together:

$$\begin{aligned} |V_{\Lambda_i}(\pi_1, \pi_2, \mathbf{s}, \boldsymbol{\lambda}) - V_{\Lambda_i}(\pi_3, \pi_4, \mathbf{s}, \boldsymbol{\lambda})| & \leq 2n\mathcal{R}_{max}(1 + \gamma(1 - \gamma)^{-1})\rho_{TV}((\pi_1, \pi_2), (\pi_3, \pi_4)) \\ & \quad + \gamma \max_{\mathbf{s}, \boldsymbol{\lambda}} |V_{\Lambda_i}(\pi_1, \pi_2, \mathbf{s}, \boldsymbol{\lambda}) - V_{\Lambda_i}(\pi_3, \pi_4, \mathbf{s}, \boldsymbol{\lambda})| \end{aligned}$$

Taking the maximum over $\mathbf{s}, \boldsymbol{\lambda}$ on the left hand-side and rearranging terms finally yields:

$$\begin{aligned} |V_{\Lambda_i}(\pi_1, \pi_2) - V_{\Lambda_i}(\pi_3, \pi_4)| & \leq \max_{\mathbf{s}, \boldsymbol{\lambda}} |V_{\Lambda_i}(\pi_1, \pi_2, \mathbf{s}, \boldsymbol{\lambda}) - V_{\Lambda_i}(\pi_3, \pi_4, \mathbf{s}, \boldsymbol{\lambda})| \\ & \leq 2n(1 - \gamma)^{-1}\mathcal{R}_{max}(1 + \gamma(1 - \gamma)^{-1})\rho_{TV}((\pi_1, \pi_2), (\pi_3, \pi_4)) \\ & = 2n(1 - \gamma)^{-2}\mathcal{R}_{max}\rho_{TV}((\pi_1, \pi_2), (\pi_3, \pi_4)) \end{aligned}$$

which yields the desired continuity result. \square

B Experiments: details and complete set of results

B.1 Description of the n-player market setting and of the merchant agents on a shared policy

We implemented a simulator of a market where **merchant** agents i offer prices $\mathbf{p}_{buy,t}^{(i)}$, $\mathbf{p}_{sell,t}^{(i)}$ to **customers** at which they are willing to *buy* and *sell* a certain good, for example coffee, from/to them. A given merchant i cannot observe the prices that his competitors $j \neq i$ are offering to customers, hence the partially observed setting.

There exists a **reference facility** that all merchants and customers can observe and can transact with at buy/sell prices $\mathbf{p}_{buy,t}^*$, $\mathbf{p}_{sell,t}^*$ publicly available at all times. Consequently, if a merchant offers to a customer a price less attractive than the reference price, the customer will prefer to transact with the reference facility instead. $\mathbf{p}_{buy,t}^*$, $\mathbf{p}_{sell,t}^*$ are assumed to be of the form $\mathbf{p}_{buy,t}^* = \mathbf{m}_t^* - \boldsymbol{\delta}_t^*$, $\mathbf{p}_{sell,t}^* = \mathbf{m}_t^* + \boldsymbol{\delta}_t^*$, where both \mathbf{m}_t^* , $\boldsymbol{\delta}_t^*$ have Gaussian increments over each timestep and $\boldsymbol{\delta}_t^* \geq 0$.

A **merchant i 's inventory** $q_t^{(i)}$ is the net quantity of good that remains in his hands as a result of all transactions performed with customers and the reference facility up to time t . We assume that it is permitted to sell on credit, so that inventory $q_t^{(i)}$ can be negative.

We have denoted the prices in bold letters since these prices are in fact functions of the quantity q that is being transacted, for example $\mathbf{p}_{buy,t}^{(i)} \equiv q \rightarrow p_{buy,t}^{(i)}(q)$. In order to simplify the setting, we assume that **merchants' actions** $\mathbf{a}_t^{(i)}$ only consist in i) specifying multiplicative buy/sell factors $\epsilon_{t,b}^{(i)}$, $\epsilon_{t,s}^{(i)} \in [-1, 1]$ on top of the reference curve to generate price curves: $\mathbf{p}_{buy,t}^{(i)} := \mathbf{p}_{buy,t}^*(1 + \epsilon_{t,b}^{(i)})$, $\mathbf{p}_{sell,t}^{(i)} := \mathbf{p}_{sell,t}^*(1 + \epsilon_{t,s}^{(i)})$ and ii) specifying a fraction $h_t^{(i)} \in [0, 1]$ of current inventory $q_t^{(i)}$ to transact at the reference facility, so that $\mathbf{a}_t^{(i)} = (\epsilon_{t,b}^{(i)}, \epsilon_{t,s}^{(i)}, h_t^{(i)}) \in [-1, 1]^2 \times [0, 1]$. The **merchant's state** $\mathbf{s}_t^{(i)} \in \mathbb{R}^d$ with $d \sim 500$ consist in the reference price and his recent transaction history with all customers, in particular his inventory.

Merchants' rewards depend on other merchant's prices and consist in the profit made as a result of i) transactions performed with customers and the reference facility and ii) the change in inventory's value due to possible fluctuations of the reference price.

Customers are assumed at every point in time t to either want to buy or sell with equal probability a certain quantity. We split 500 customers into 10 **customer clusters**, cluster $i \in [1, 10]$ being associated to quantity i . For example, a customer belonging to cluster 5 will generate transactions of quantity 5.

Types and supertypes. In our setting, merchants differ by 1) their **connectivity** to customers (they can transact only with connected customers) and 2) their **inventory tolerance** factor ξ_i , which penalizes holding a large inventory by adding a term $-\xi_i |q_t^{(i)}|$ to their reward. We define the **supertype** Λ_i as a **vector of size 12**: 10 probabilities of being connected to customers belonging to the 10 customer clusters, plus the mean and standard deviation of the normal distribution generating the merchant’s inventory tolerance coefficient ξ_i ¹. In a given episode, a merchant may be connected differently to customers in the same cluster, however he has the same probability to be connected to them. That means that the **type** λ_i sampled probabilistically at the beginning of each episode is a vector of size 11: 10 entries in $[0, 1]$ corresponding to the sampled fractions of connected customers in each one of the 10 clusters, and 1 inventory tolerance factor. For example, if a merchant has in its supertype a probability 30% to be connected to customers in cluster 5, then each one of the 50 binary connections between the merchant and customers of cluster 5 will be sampled independently at the beginning of the episode as a Bernoulli random number with associated probability 30%, and the resulting fraction of connected customers is recorded in λ_i .

Calibration targets. We consider calibration targets of two different types. The **market share** of a specific merchant i is defined as the fraction of the sum of all customers’ transaction quantities (over an episode) that merchant i has obtained. Note that the sum of market share over merchant’s doesn’t necessarily sum to 1 since customers can transact with the reference facility if the merchant’s prices are not attractive enough. The **transaction distribution** is defined as percentiles of the distribution - over an episode - of transaction quantities per timestep received by a merchant as a result of his interactions with all customers.

B.2 RL calibrator agent

As described in section 3, the state of the RL calibrator is the current supertype profile Λ and its action is a supertype profile increment $\delta\Lambda$. In section B.1, we described the supertype Λ_i for each merchant as a vector of size 12, and in section 4 we mentioned that we conducted experiments using 2 distinct supertypes for the 5-10 merchant agents (see also section B.3 for a more detailed description). As a result, both the calibrator’s state Λ and action $\delta\Lambda$ consist of the 12 supertype entries for 2 distinct supertypes, i.e. 24 real numbers. In our experiments, we set the standard deviation of the normal distribution associated to inventory tolerance of supertype 1 to be zero since supertype 1 is associated to 1 merchant only, which reduces the size to 23 real numbers. The corresponding ranges for the parameters $(\Lambda_i(j))_{j=1..12}$ in the RL calibrator’s policy action and state spaces are reported in table 1.

Table 1: RL calibrator state and action spaces.

Supertype parameter flavor j	state $\Lambda_i(j)$ range	action $\delta\Lambda_i(j)$ range
customer cluster connectivity probability	$[0, 1]$	$[-1, 1]$
inventory tolerance Gaussian mean	$[0, 5]$	$[-5, 5]$
inventory tolerance Gaussian stDev	$[0, 2]$	$[-2, 2]$

As mentioned in section 3, the calibrator agent’s reward r_b^{cal} associated to an episode b is given by

$$r_b^{cal} = \sum_{k=1}^K w_k \overbrace{\ell_k^{-1}(f_*^{(k)} - f_{cal}^{(k)}((z_{t,b})_{t \geq 0}))}^{r_b^{(k)}} \quad (7)$$

We give in table 3 a breakdown of these sub-objectives for each experiment (for each experiment, all K sub-objectives are required to be achieved simultaneously, cf. equation (7) above). Table 3 is

¹in experiments of section B.3, we set the standard deviation of the normal distribution associated to inventory tolerance of supertype 1 to be zero since supertype 1 is associated to 1 merchant only

associated with reward functions mentioned below, where we denote $m_{super_1} = m_{super_1}((z_t)_{t \geq 0})$ the market share of supertype 1 observed throughout an episode, m_{total} the sum of all merchants' marketshares, $\hat{v}_{super_j}(p)$ the observed $(10p)^{th}\%$ percentile of supertype j 's transaction distribution per timestep.

In experiment 1, $r = (1 + r^{(1)} + 0.2r^{(2)})^{-1}$, with $v_{super_1} = [8, 8, 8, 9, 9, 9, 10, 10, 10]$, $r^{(1)} = \frac{1}{2}(\max(0.15 - m_{super_1}, 0) + \max(0.8 - m_{total}, 0))$, $r^{(2)} = \frac{1}{9} \sum_{p=1}^9 |v_{super_1}(p) - \hat{v}_{super_1}(p)|$.

In experiment 2/3, $r = (1 + r^{(1)} + 0.2r^{(2)} + 0.2r^{(3)})^{-1}$, with $v_{super_1} = [8, 8, 8, 9, 9, 9, 10, 10, 10]$, $v_{super_2} = [2, 3, 3, 4, 5, 5, 6, 6, 7]$, $r^{(1)} = \frac{1}{2}(\max(0.15 - m_{super_1}, 0) + \max(0.8 - m_{total}, 0))$, $r^{(j+1)} = \frac{1}{9} \sum_{p=1}^9 |v_{super_j}(p) - \hat{v}_{super_j}(p)|$, $j \in \{1, 2\}$.

In experiment 4, $r = (1 + r^{(1)} + r^{(2)})^{-1}$, with $r^{(1)} = |0.25 - m_{super_1}|$, $r^{(2)} = \max(0.8 - m_{total}, 0)$.

In experiment 5, $r = (1 + r^{(1)} + r^{(2)})^{-1}$, with $r^{(1)} = |0.4 - m_{super_1}|$, $r^{(2)} = |0.8 - m_{total}|$.

B.3 Details on experiments

Experiments were conducted in the RLlib multi-agent framework Liang *et al.* (2018), ran on AWS using a EC2 C5 24xlarge instance with 96 CPUs, resulting in a training time of approximately 1 day per experiment.

The 5 experiments we conducted are described in table 2, with a calibration target breakdown in table 3 (see section B.1 for a description of the market setting and merchant agents, and section B.2 for a description of the RL calibrator agent's state, actions and rewards). For example, according to table 3, in experiment 1, we calibrate 23 parameters altogether in order to achieve 11 calibration targets simultaneously. As mentioned in section 4, in all experiments, merchant 1 was assigned supertype 1, and all $n - 1$ other merchants were assigned supertype 2.

Shared Policy and calibrator's policy. Both policies were trained jointly according to algorithm 1 using Proximal Policy Optimization Schulman *et al.* (2017), an extension of TRPO Schulman *et al.* (2015). We used configuration parameters in line with Schulman *et al.* (2017), that is a clip parameter of 0.3, an adaptive KL penalty with a KL target of 0.01 and a learning rate of 10^{-4} . We found that entropy regularization was not specifically helpful in our case. Episodes were taken of length 60 time steps with a discount factor of 1, using $B = 90$ parallel runs in between policy updates (for both policies). As a result, each policy update was performed with a batch size of $n \cdot 60 \cdot 90$ timesteps for the shared policy, and $3 \cdot 90$ timesteps for the calibrator's policy, as we allowed the calibrator to take 3 actions per episode (that is, updating the supertype profile Λ 3 times), together with 30 iterations of stochastic gradient descent. We used for each policy a fully connected neural net with 2 hidden layers, 256 nodes per layer, and tanh activation. Since our action space is continuous, the outputs of the neural net are the mean and stDev of a standard normal distribution, which is then used to sample actions probabilistically (the covariance matrix across actions is chosen to be diagonal).

Bayesian optimization baseline. We used Bayesian optimization to suggest a next supertype profile Λ to try next, every M training iterations of the shared policy. That is, every M training iterations, we record the calibrator's reward as in section B.2, and use Bayesian optimization to suggest the next best Λ to try. We empirically noticed that if M was taken too low ($M \sim 10$), the shared policy couldn't adapt as the supertype profile changes were too frequent (and potentially too drastic), thus leading to degenerate behaviors (e.g. merchants not transacting at all). We tested values of $M = 10$, $M = 50$, $M = 100$, $M = 200$, and opted for $M = 100$ as we found it was a good trade-off between doing sufficiently frequent supertype profile updates and at the same time giving enough time to the shared policy to adapt. We chose an acquisition function of upper confidence bound (UCB) type Srinivas *et al.* (2016). Given the nature of our problem where agents on the shared policy need to be given sufficient time to adapt to a new supertype profile choice Λ , we opted for a relatively low UCB exploration parameter of $\beta = 0.5$, which we empirically found yielded a good trade-off between exploration and exploitation (taking high exploration coefficient can yield drastic changes in the supertype profile space, which can prevent agents to learn correctly an equilibrium). Taking an acquisition function of expected improvement type yielded a similar performance, cf. figure 4. The covariance function of the Gaussian process was set to a Matern kernel with $\nu = 2.5$.

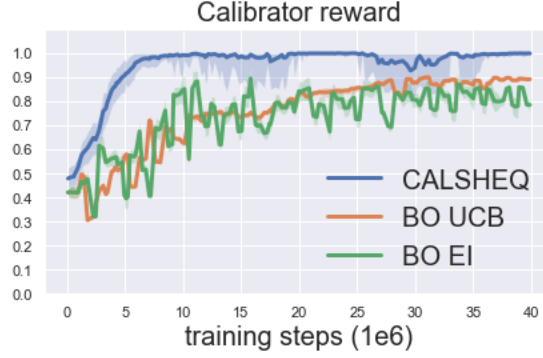


Figure 4: Calibrator Reward during training - Experiment 1 - BO UCB with exploration parameter $\beta = 0.5$, BO Expected Improvement (EI).

Table 2: Summary of experiment configuration.

Experiment #	# Merchant Agents	Budget # Training Steps (10^6)	# distinct Supertypes	# Supertype parameters to be calibrated	Total # Calibration Targets
1	5	40	2	20	11
2	5	40	2	20	20
3	10	20	2	20	20
4	10	20	2	23	2
5	5	40	2	23	2

Table 3: Calibration target breakdown

Experiment #	# Calibration Targets	Calibration Target Type
1	9	transaction quantity distribution supertype 1 percentiles 10% – 90% target 8, 8, 8, 9, 9, 9, 10, 10, 10
	2	market share supertype 1 $\geq 15\%$ + total $\geq 80\%$
2	18	transaction quantity distribution Supertypes 1+2 supertype 1 - percentiles 10% – 90% target 8, 8, 8, 9, 9, 9, 10, 10, 10 supertype 2 - percentiles 10% – 90% target 2, 3, 3, 4, 5, 5, 6, 6, 7
	2	market share supertype 1 $\geq 15\%$ + total $\geq 80\%$
3	18	transaction quantity distribution Supertypes 1+2 supertype 1 - percentiles 10% – 90% target 8, 8, 8, 9, 9, 9, 10, 10, 10 supertype 2 - percentiles 10% – 90% target 2, 3, 3, 4, 5, 5, 6, 6, 7
	2	market share supertype 1 $\geq 15\%$ + total $\geq 80\%$
4	1	market share supertype 1 = 25%
	1	total market share $\geq 80\%$
5	1	market share supertype 1 = 40%
	1	total market share = 80%

B.4 Complete set of experimental results associated to section 4

In this section we display the complete set of results associated to figures shown in section 4. We display in figure 5 the rewards of all agents during training (calibrator, merchant on supertype 1 and $n - 1$ merchants on supertype 2) for experiments 1-5 previously described. In figures 6-10 we display the calibration fits for all calibration targets described in table 3 (we reiterate that for each experiment,

all calibration targets are required to be achieved simultaneously). In figures 11-15 we display the calibrated parameters associated to the calibration fits, that is the parameters in supertypes 1 and 2 (customer connectivity probability and inventory tolerance Gaussian mean and stDev) that allow to reach the calibration targets. As discussed in section 4, *CALSHEQ* outperforms BO in terms of efficiency, accuracy of the fit, and smoothness. The shaded areas correspond to 1 stDev, computed according to the so-called range rule $\frac{(\max - \min)}{4}$. In the case of *CALSHEQ*, we plot the mean of the calibration targets and calibrated parameters over the B episodes.



Figure 5: Rewards during training, averaged over episodes B - Calibrator (**Top**), Supertypes 1/2 (**Mid/Bottom**) - experiments 1-2-3-4-5, respectively 5-5-10-10-5 agents. *CALSHEQ* (ours) and baseline (Bayesian optimization). Shaded area represents ± 1 stDev.

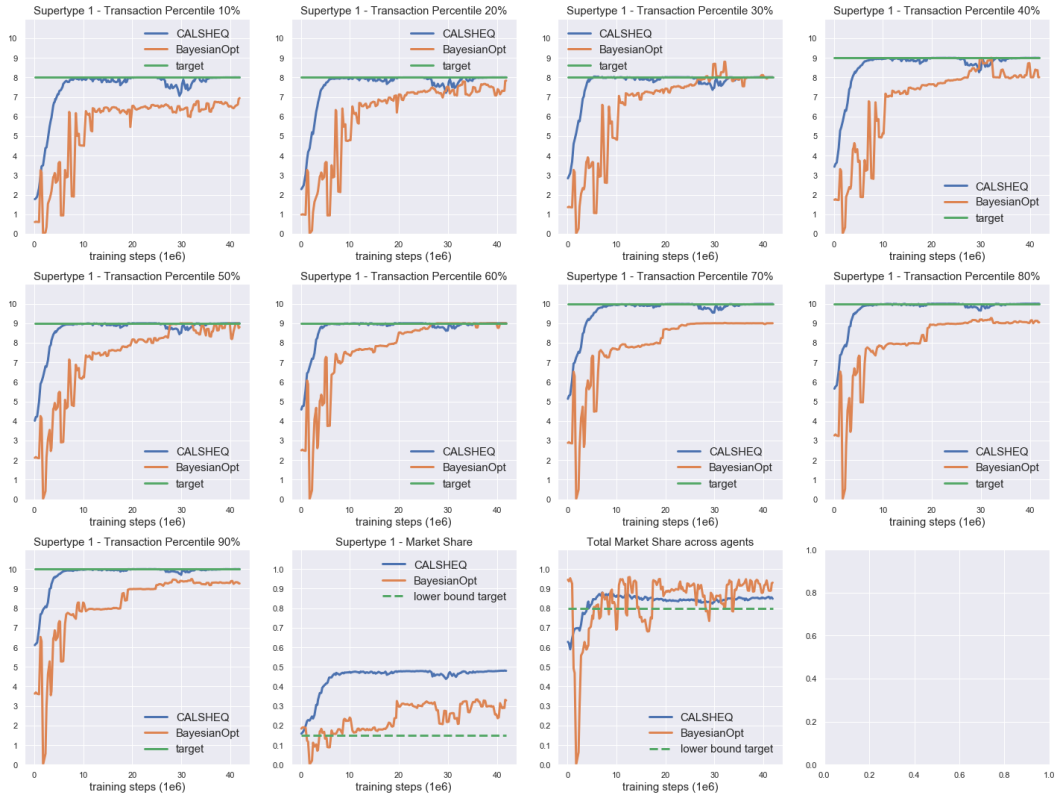


Figure 6: Experiment 1 - Calibration target fit for transaction quantity distribution percentile and Market Share during training, averaged over episodes B . Dashed line target indicates that the constraint was set to be greater than target (not equal to it). *CALSHEQ* (ours) and baseline (Bayesian optimization).



Figure 7: Experiment 2 - Calibration target fit for transaction quantity distribution percentile and Market Share during training, averaged over episodes B . Dashed line target indicates that the constraint was set to be greater than target (not equal to it). *CALSHEQ* (ours) and baseline (Bayesian optimization).

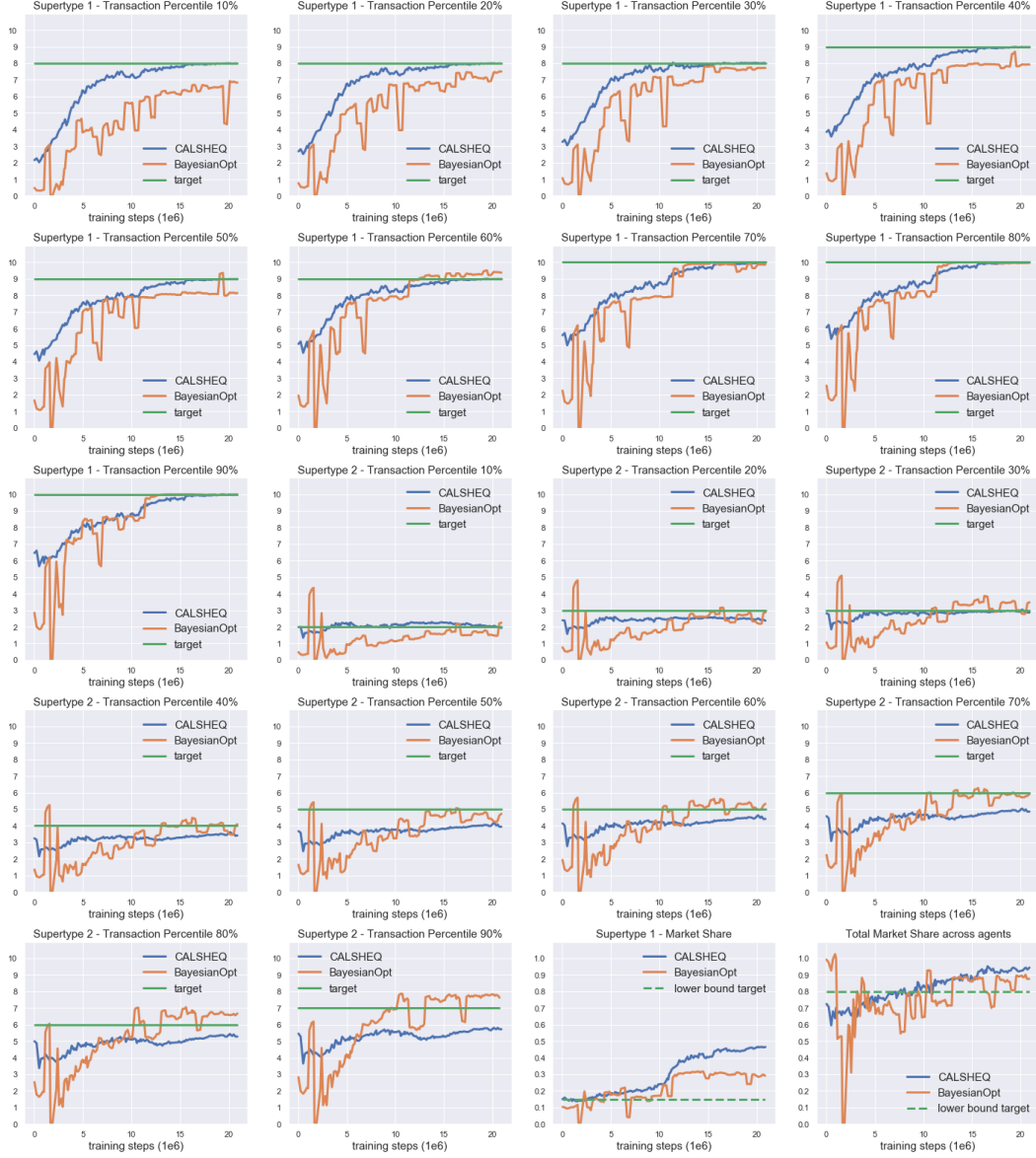


Figure 8: Experiment 3 - Calibration target fit for transaction quantity distribution percentile and Market Share during training, averaged over episodes B . Dashed line target indicates that the constraint was set to be greater than target (not equal to it). *CALSHEQ* (ours) and baseline (Bayesian optimization).

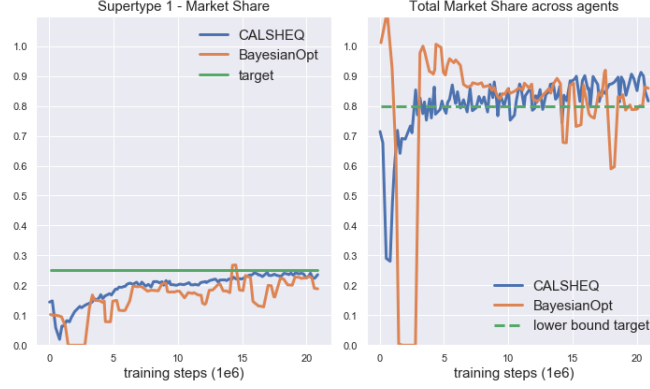


Figure 9: Experiment 4 - Calibration target fit for Market Share during training, averaged over episodes B . Dashed line target indicates that the constraint was set to be greater than target (not equal to it). *CALSHEQ* (ours) and baseline (Bayesian optimization).

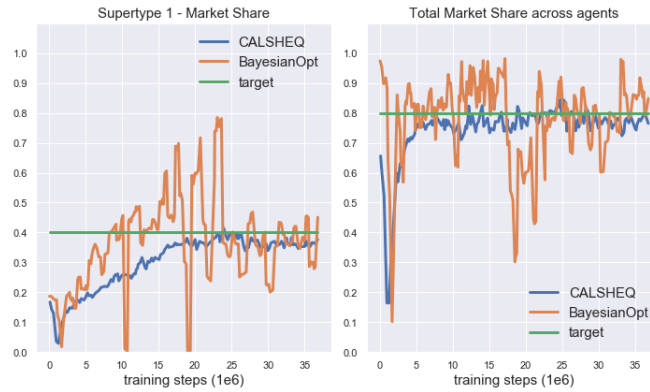


Figure 10: Experiment 5 - Calibration target fit for Market Share during training, averaged over episodes B . *CALSHEQ* (ours) and baseline (Bayesian optimization).

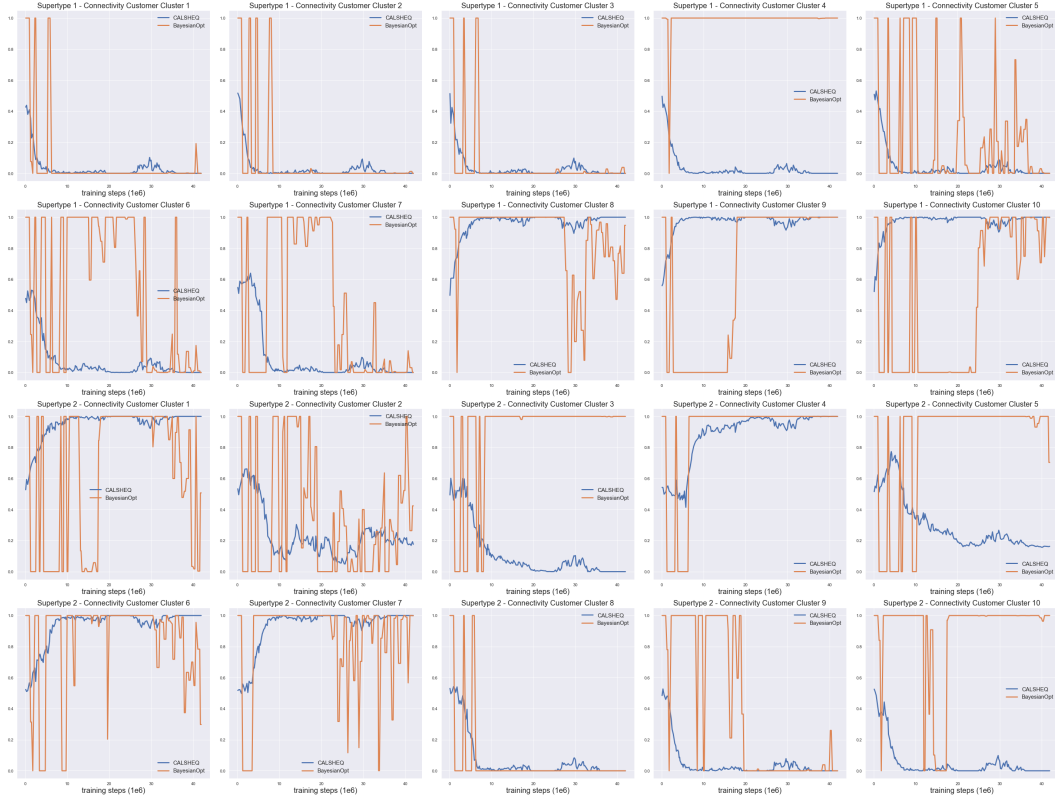


Figure 11: Experiment 1 - Calibrated parameters, averaged over episodes B . *CALSHEQ* (ours) and baseline (Bayesian optimization).

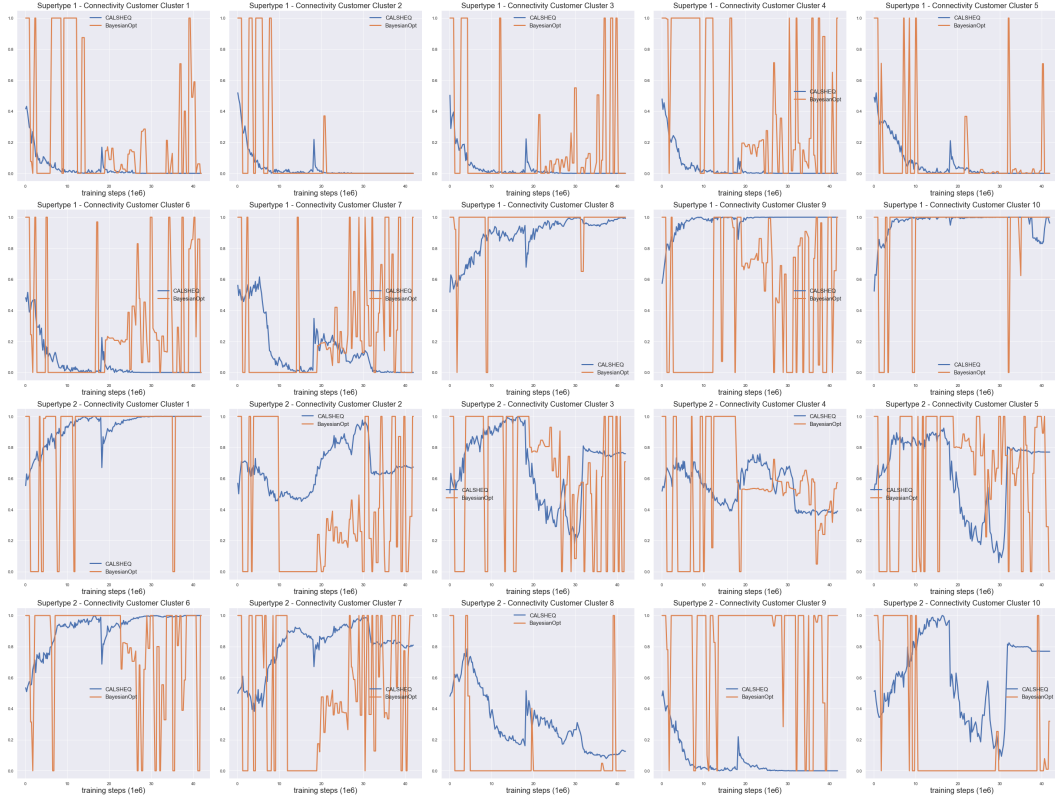


Figure 12: Experiment 2 - Calibrated parameters, averaged over episodes B . *CALSHEQ* (ours) and baseline (Bayesian optimization).

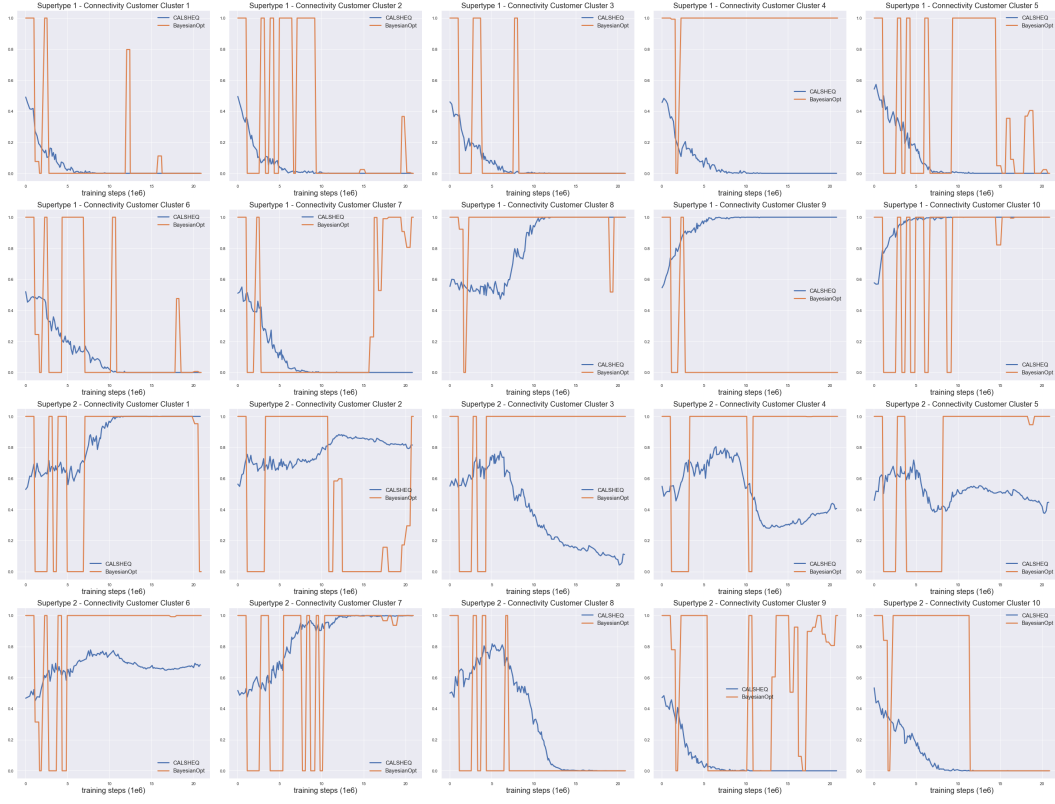


Figure 13: Experiment 3 - Calibrated parameters, averaged over episodes B . *CALSHEQ* (ours) and baseline (Bayesian optimization).



Figure 14: Experiment 4 - Calibrated parameters, averaged over episodes B . *CALSHEQ* (ours) and baseline (Bayesian optimization).

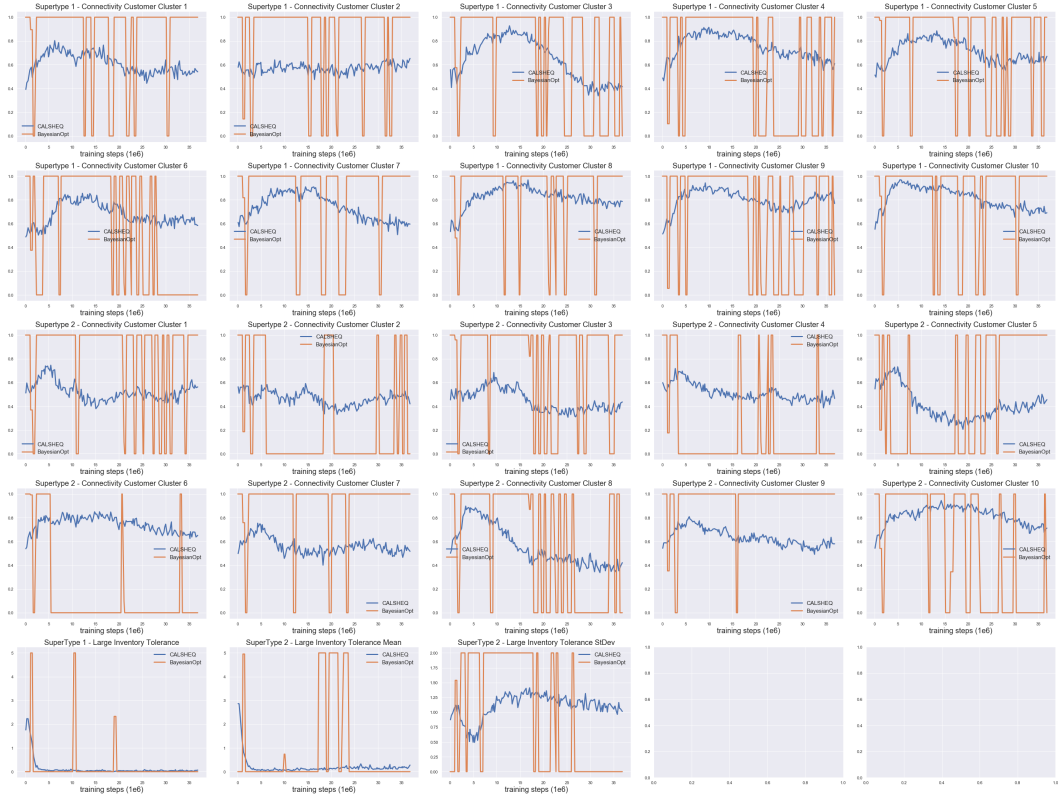


Figure 15: Experiment 5 - Calibrated parameters, averaged over episodes B . *CALSHEQ* (ours) and baseline (Bayesian optimization).